

Reciprocal Regulation of Lymphoid Tissue Development in the Large Intestine by IL-25 and IL-23

David S Donaldson, Barry M Bradford, David Artis & Neil A Mabbott

Supplimentary Methods

Supplementary Figures 1-4

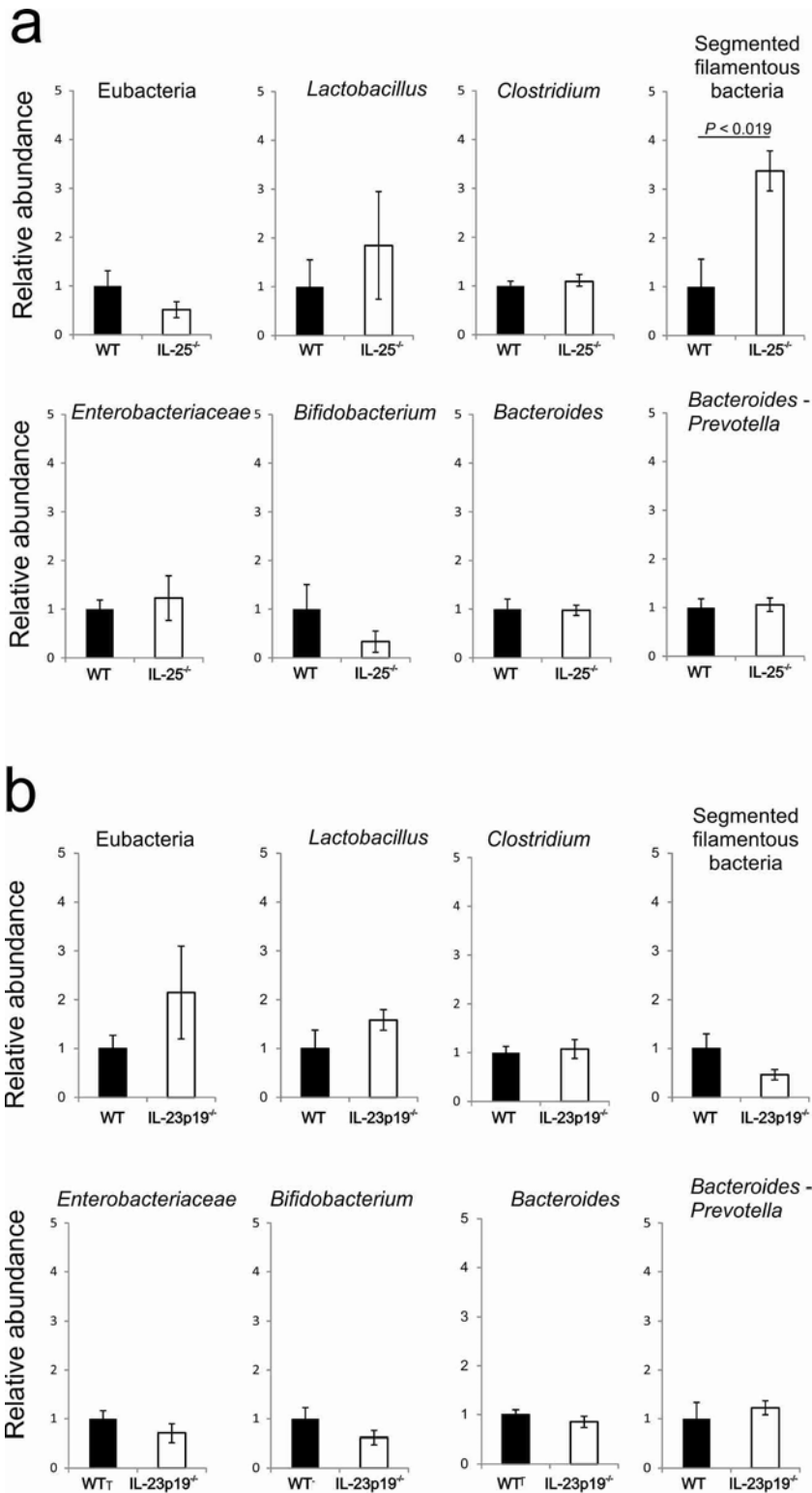
Supplementary Methods

Neutralisation of IL-17 and IL-22 in vivo. To block Peyer's patch development, pregnant mice were given an intra-peritoneal (i.p) injection of 100 µg LTβR-Ig (Biogen Idec, Weston, MA, U.S.A.) at E9-11 d. For IL-17 and IL-22 neutralisation, mice were i.p. injected with 200 µg of anti-mouse IL-17 mAb (50104) (or control rat IgG2a; 54447) every 3 d for 15 d⁵² or 100 µg of polyclonal goat anti-mouse IL-22 Ab (or control goat IgG) every 4 d for 12 d⁵³ (all R&D Systems).

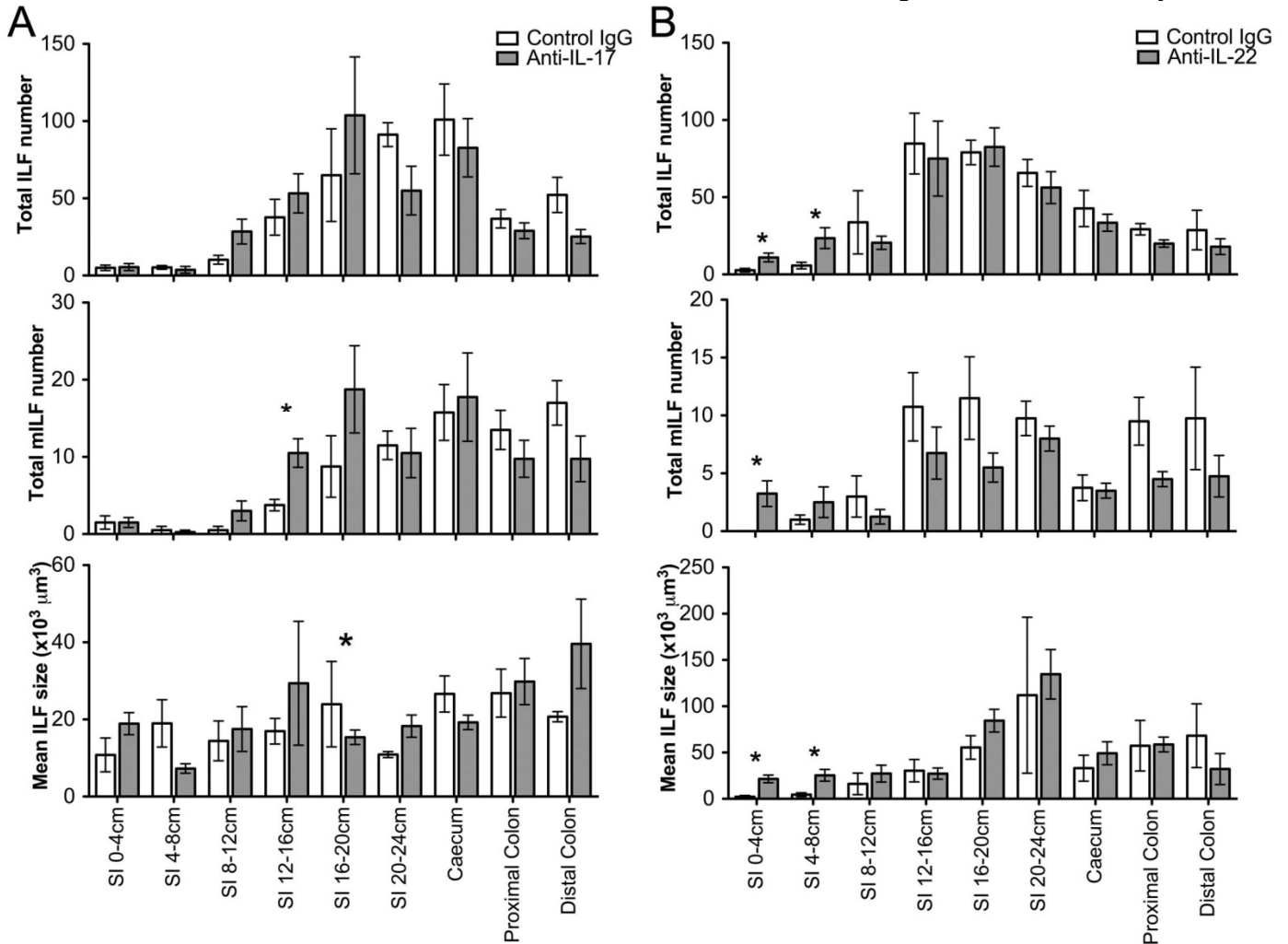
Bacterial genomic DNA extraction and qRT-PCR amplification of bacterial 16S rRNA gene sequences. The abundance of specific intestinal bacterial groups was measured by qRT-PCR as described⁵⁴. Briefly, bacterial genomic DNA was extracted from faeces (n=4/group) by use of a Qiagen stool kit (Qiagen, Manchester, UK) according to the manufacturer's instructions and using the optional high-temperature step. qRT-PCR was performed with FastStart Universal SYBR Green Master (ROX) (Roche Diagnostics GmbH, Mannheim, Germany) using a Stratagene MX3005P (Agilent Technologies, Waldbronn, Germany) and group-specific 16S rRNA gene primers (Supplementary Table 1^{54, 55}). The relative abundance of bacterial groups was then calculated between the knockout mice and their co-housed wild type controls.

References

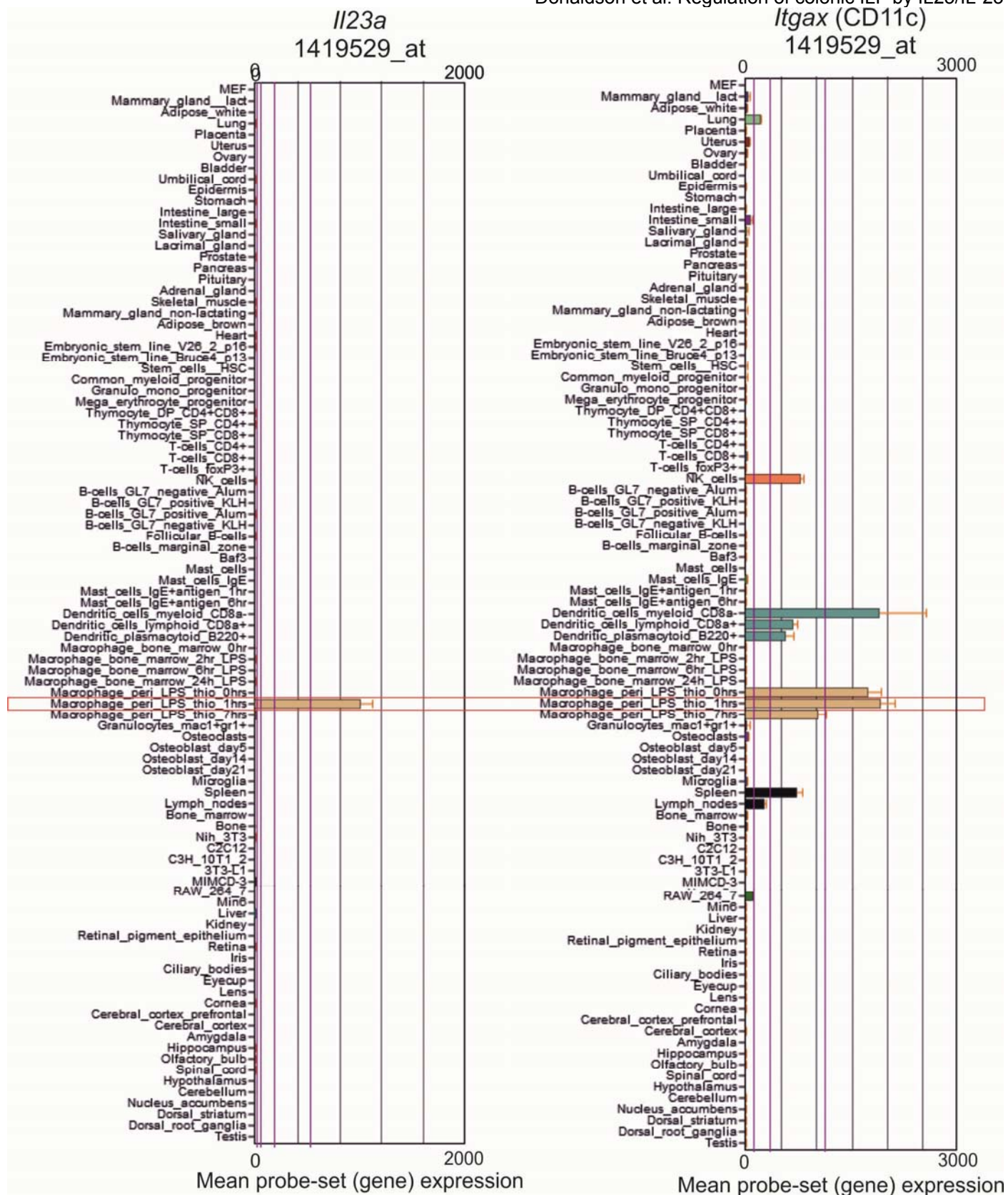
52. Pollinger, B. *et al.* Th17 cells, not IL-17+ gammadelta T cells, drive arthritic bone destruction in mice and humans. *J. Immunol.* **186**, 2602-2612 (2011).
53. Guo, H. & Topham, D.J. Interleukin-22 (IL-22) production by pulmonary Natural Killer cells and the potential role of IL-22 during primary influenza virus infection. *J. Virol.* **84**, 7750-7759 (2010).
54. Barman, M. *et al.* Enteric salmonellosis disrupts the microbial ecology of the murine gastrointestinal tract. *Infect. Immun.* **76**, 907-915 (2008).
55. Bindels, L.B. *et al.* Restoring specific lactobacilli levels decreases inflammation and muscle atrophy markers in an acute leukemia mouse model. *PLoS one* **7**, e37971 (2012).



Supplementary Figure 1: Comparison of the colonic microbiota in WT, IL-25^{-/-} and IL-23p19^{-/-} mice. Faecal samples were collected from individual mice (n = 4/group) and the microbiota analysed by qRT-PCR analysis of DNA encoding bacterial 16S rRNA. The relative abundance of each major bacterial grouping was determined in (a) IL-25^{-/-} mice and (b) IL-23p19^{-/-} mice compared to co-housed WT controls. No significant changes were observed in the overall burden and composition of the microbiota between IL-25^{-/-} or IL-23^{-/-} mice and the respective WT mice, with the exception of segmented filamentous bacteria, which was significantly increased in IL-25^{-/-} mice (Supplementary Figure 1a; $P < 0.019$, Student's *t*-test). Data represent the mean \pm SE.



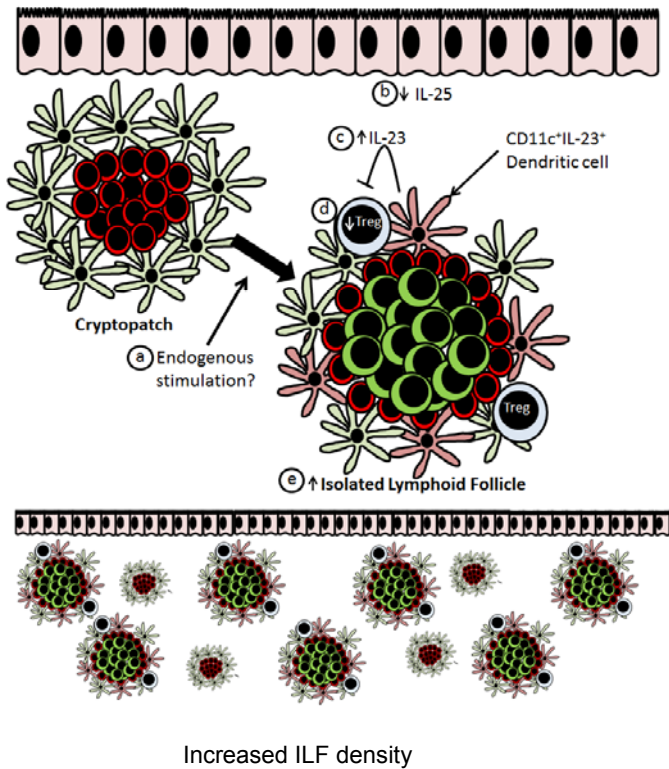
Supplementary Figure 2: Neutralisation of IL-17 or IL-22 during isolated lymphoid follicle (ILF) development does not recapitulate the phenotype of *IL-23p19^{-/-}* mice. Pregnant mice were injected with LT β R-Ig to block Peyer's patch development and enhance ILF development in the progeny. Progeny mice were administered neutralising (a) anti-IL-17 or (b) anti-IL-22, or respective control Ig, between 14 and 28 d after birth. Mice were culled at 30 d after birth and the alternate 4 cm sections of small intestine (SI) and the whole large intestine were wholemount immunostained for B220 and CD35 to identify ILF and mILF respectively. The total number of ILF and mILF and the mean ILF size were determined by microscopy (n=4). Statistical differences were determined by students t-test (* represents p<0.05).



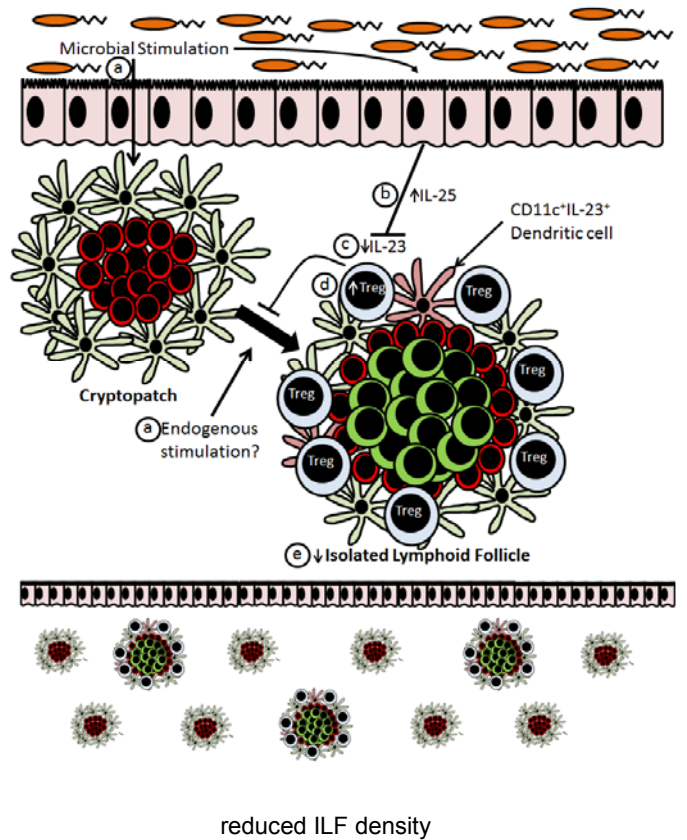
Supplementary Figure 3: *IL23a* expression is restricted to specific populations of *CD11c*⁺ mononuclear phagocytes

Expression profile of *IL23a* (left, which encodes IL-23; Affymetrix probe set ID 1419529_at) and *Itgax* (right, which encodes CD11c; Affymetrix probe set ID 1419128_at) across a wide range of microarray data sets (>200) representing 95 distinct mouse tissues and cell-lineages. All sample analysis was performed on the Affymetrix MOE430 2.0 expression array. Data were analysed using the GNF1M Mouse tissue atlas (<http://biogps.gnf.org>). The normalised, mean gene expression level data for each tissue and cell type are shown. These data show that across this data set IL-23 is only expressed by a restricted population of *CD11c*⁺ mononuclear phagocytes (red box).

a Germ-Free



b Conventionalised



Supplementary Figure 4: Mechanism of how colonisation with the microbiota leads to reduced Isolated lymphoid follicle (ILF) development. **(a)** In germ-free mice, ILF development from cryptopatches is stimulated by an unknown mechanism, potentially through endogenous stimulation (a). Due to the absence of the microbiota, IL-25 production is diminished (b). This leads to increased IL-23 secretion by CD11c⁺ cells within colonic ILF (c). IL-23 may suppress regulatory T cell (Treg) development, reducing Treg numbers (d). The absence of Treg-mediated suppression of ILF development results in increased numbers of ILF (e). **(b)** Following conventionalisation, ILF can be stimulated by both microbial and endogenous stimulation (a). However, in the presence of the microbiota, epithelial IL-25 secretion is increased (b). This leads to reduced IL-23 secretion from CD11c⁺ cells (c). The reduction in IL-23 secretion permits the expansion of Treg that are capable of suppressing ILF development (d). This suppression of ILF development leads to reduced ILF numbers (e).